Journal of Pharmacological Sciences 132 (2016) 154–161

Contents lists available at ScienceDirect

Journal of Pharmacological Sciences

journal homepage: www.elsevier.com/locate/jphs

Full paper

Salubrinal improves mechanical properties of the femur in osteogenesis imperfecta mice

Shinya Takigawa [a, b], Brian Frondorf [a], Shengzhi Liu [a, c], Yang Liu [a, c], Baiyan Li [c], Akihiro Sudo [b], Joseph M. Wallace [a], Hiroki Yokota [a], Kazunori Hamamura [a, d, *]

[a] Department of Biomedical Engineering, Indiana University Purdue University Indianapolis, Indianapolis, IN, USA
[b] Department of Orthopaedic Surgery, Mie University Graduate School of Medicine, Mie, Japan
[c] Department of Pharmacology, School of Pharmacy, Harbin Medical University, Harbin, China
[d] Department of Pharmacology, School of Dentistry, Aichi-Gakuin University, Nagoya, Japan

ARTICLE INFO

Article history:
Received 10 July 2016
Received in revised form
17 September 2016
Accepted 25 September 2016
Available online 1 October 2016

Keywords:
Salubrinal
Osteogenesis imperfecta
Osteoclasts
Bone marrow derived cells
Mechanical test

ABSTRACT

Salubrinal is an agent that reduces the stress to the endoplasmic reticulum by inhibiting de-phosphorylation of eukaryotic translation initiation factor 2 alpha (eIF2α). We and others have previously shown that the elevated phosphorylation of eIF2α stimulates bone formation and attenuates bone resorption. In this study, we applied salubrinal to a mouse model of osteogenesis imperfecta (Oim), and examined whether it would improve Oim's mechanical property. We conducted *in vitro* experiments using RAW264.7 pre-osteoclasts and bone marrow derived cells (BMDCs), and performed *in vivo* administration of salubrinal to Oim (+/−) mice. The animal study included two control groups (wildtype and Oim placebo). The result revealed that salubrinal decreased expression of nuclear factor of activated T cells cytoplasmic 1 (NFATc1) and suppressed osteoclast maturation, and it stimulated mineralization of mesenchymal stem cells from BMDCs. Furthermore, daily injection of salubrinal at 2 mg/kg for 2 months made stiffness (N/mm) and elastic module (GPa) of the femur undistinguishable to those of the wildtype control. Collectively, this study supported salubrinal's beneficial role to Oim's femora. Unlike bisphosphonates, salubrinal stimulates bone formation. For juvenile OI patients who may favor strengthening bone without inactivating bone remodeling, salubrinal may present a novel therapeutic option.

1. Introduction

Osteogenesis Imperfecta (OI) is a rare bone disorder, characterized by brittle bone prone to fracture (1,2). There are at least 8 types of OI (types I–VIII). The majority of affected persons (85–90%) have mutations in the COL1A1 and COL1A2 genes (type I collagen genes) (3,4). The incidence of OI is estimated to be one per 20,000 live births, and a high rate of bony fracture occurs mostly in childhood (5). With adaptive equipment such as metal rods, wheelchairs, splints etc., many individuals with moderate/severe OI can obtain a certain degree of autonomy. Existing drugs such as bisphosphonates for treating osteoporosis are shown to partially alleviate OI symptoms (6). However, bisphosphonates do not stimulate bone formation (7,8). They induce side effects such as gastrointestinal irritation/ulcer (when given orally), uveitis (eye inflammation), and hypocalcemia (9). Inhibition of receptor activator of nuclear factor kappa-B ligand (RANKL) by neutralizing antibody is reported to improve geometric and biomechanical properties of bone in juvenile OI mice, but it did not decrease fracture incidence (10). Thus, there is a pressing need to develop a novel treatment strategy, in particular, using drugs that can increase mechanical properties (11,12).

Since OI is induced by genetic mutations that lead to protein misfolding (13), we focused in this study on a signaling pathway linked to protein misfolding, by inhibiting de-phosphorylation of eIF2α (eukaryotic translation initiation factor 2 alpha). Protein misfolding, induced by a genetic mutation in type I collagen gene, is

* Corresponding author. Department of Pharmacology, School of Dentistry, Aichi-Gakuin University, 1-100 Kusumoto-Cho, Chikusa-Ku, Nagoya 464-8650, Japan. Fax: +81 52 752 5988.
E-mail address: hamak@dpc.agu.ac.jp (K. Hamamura).
Peer review under responsibility of Japanese Pharmacological Society.

http://dx.doi.org/10.1016/j.jphs.2016.09.006

expected to induce stress to the endoplasmic reticulum and leads to apoptosis of bone-forming osteoblasts (14,15). The elevation of phosphorylated eIF2α is shown to alleviate protein misfolding responses, and a synthetic compound, salubrinal (479.8 Da; $C_{21}H_{17}Cl_3N_4OS$), is known to elevate the phosphorylation level of eIF2α by suppressing protein phosphatase 1, a specific phosphatase to eIF2α (16).

We have previously shown that salubrinal is able to inhibit development of bone-resorbing osteoclasts by in-activating NFATc1 transcription factor (17,18), and stimulate development of bone-forming osteoblasts by activating ATF4 transcription factor (17,19). Furthermore, it is reported that salubrinal-driven upregulation of ATF4 increases osteocalcin (17). Currently, few existing drugs for treatment of osteoporosis are able to function both as bone-forming and resorption-inhibitory agents. Neutralizing antibody to RANKL and bisphosphonates may block bone resorption but they do not stimulate bone formation. PTH (parathyroid hormone) may stimulate bone formation, but it does not inhibit bone resorption (20,21) and has a black box warning prohibiting use in children.

In this study, we used an established pre-osteoblast line, primary bone marrow derived cells (BMDCs), and the mouse model of osteogenesis imperfecta (Oim mice), and evaluated the effect of salubrinal on development of osteoclasts and osteoblasts as well as mechanical properties of the femur of Oim mice.

2. Materials and methods

2.1. Cell culture

RAW264.7 pre-osteoclasts, as well as mouse bone marrow derived cells isolated from the femur and tibia of wildtype mice, were cultured in αMEM with 10% FBS and antibiotics. Furthermore, mouse bone marrow derived cells (MBMCs) were harvested from Oim mice, and mesenchymal stem cells were isolated for culture. They were grown in an osteogenic medium (100 μM ascorbic acid, and 2 mM beta glycerol phosphate) for 4 weeks. The effect of salubrinal on mineralization was evaluated using Alizarin red S staining (Sigma, St. Louise, MO, USA). Salubrinal (R&D systems, Minneapolis, MN, USA) was given to those cells at a dose of 5 or 10 μM. Salubrinal's concentration of 10 μM *in vitro* was selected based on its efficacy as a regulator of eIF2α phosphorylation as well as non-toxicity to the cells in this study.

2.2. qPCR and Western blotting

Reverse transcription was conducted using total RNA and a high-capacity cDNA reverse transcription kit (Applied Biosystems, Carlsbad, CA, USA). Quantitative real-time PCR was performed using Power SYBR green PCR master mix kits (Applied Biosystems). The mRNA level of NFATc1 was determined with GAPDH as an internal control. The PCR primers were: NFATc1 (5′-GGTGCTGTCTGGCCATAACT-3′, 5′-GCGGAAAGGTGGTATCTCAA-3′); and GAPDH (5′-TGCACCACCAACTGCTTAG-3′ and 5′-GGATGCAGGGATGATGTTC-3′).

Western blotting was conducted using 10–12% SDS gels and PVDF transfer membranes (Millipore, Billerica, MA, USA). Protein samples were isolated using a RIPA buffer. We used primary antibodies specific to eIF2α and p-eIF2α (Cell Signaling, Danvers, MA, USA), NFATc1 (Santa Cruz Biotechnology, Santa Cruz, CA, USA), as well as a secondary antibody conjugated with horseradish peroxidase (Cell Signaling). The level of proteins was detected using a SuperSignal west femto maximum sensitivity substrate (Thermo Scientific, Waltham, MA, USA), and the level of β-actin (Sigma) was employed as a control.

2.3. Osteoclastogenesis and TRAP (tartrate-resistant acid phosphatase) staining

RAW264.7 cells were cultured for 4 days in a 96-well plate (0.5×10^4 cells/well) with 50 ng/ml recombinant murine receptor activator of nuclear factor kappa-B ligand (RANKL; PeproTech, Rocky Hills, NC, USA) in the presence and absence of 10 μM salubrinal. Mouse bone marrow derived cells were cultured with 10 ng/ml of a recombinant murine macrophage colony-stimulating factor (M-CSF; PeproTech) for 3 days in 12-well plates. The surface-attached cells were then used as osteoclast precursors. These precursors were cultured with 10 ng/ml M-CSF and 50 ng/ml RANKL in the presence and absence of 10 or 20 μM salubrinal (18). TRAP staining was conducted using an acid phosphatase leukocyte kit (Sigma) (18). The number of TRAP-positive cells containing three or more nuclei was determined.

2.4. Alizarin red S staining

BMDCs, grown in the osteogenic medium, were washed with PBS twice and fixed with 60% isopropanol for 1 min at room temperature, followed by rehydration with distilled water for 3 min. They were then stained with 1% Alizarin red S for 3 min and washed with distilled water (17).

2.5. Administration of salubrinal to Oim mice

This study employed 32 female mice in total (6 weeks, ~20 g; Jackson Laboratory, Bar Harbor, ME, USA), including 12 wildtype mice (B6C3Fe/J) and 20 Oim mice (+/−; B6C3Fe a/a-Col1a2^{OIM}/J). Oim mice have a spontaneous mutation in the pro-alpha2 chain of type I collagen. All procedures performed in this study were approved by the Indiana University Animal Care and Use Committee and were in compliance with the *Guiding Principles in the Care and Use of Animals* endorsed by the American Physiological Society. Four to five mice were housed together in a cage. Animals were fed with standard laboratory chow and water *ad libitum*, and they were allowed to acclimate for 1 week before experimentation. Three animal groups were used, in which Group 1 consisted of 12 wildtype mice as a normal control. Groups 2 and 3 employed 9 and 11 Oim mice as a placebo control and salubrinal administration, respectively. Mice in group 3 received daily subcutaneous administration of salubrinal at a dose of 2 mg/kg. This dose was chosen based on a separate study using a mouse model of postmenopausal osteoporosis (data unpublished). Mice in group 2 (placebo control) received daily injection of the vehicle. After mice were euthanized, the right femur of each mouse was harvested, stripped of soft tissue, wrapped in phosphate buffered saline (PBS)-soaked gauze and frozen at −20 °C until needed.

2.6. Dual-energy X-ray absorptiometry (DEXA), micro computed tomography (μCT) and mechanical testing

Prior to sacrificing animals (16 weeks old), we conducted radiographic measurements of the femur, tibia, humerus, ulna, and lumber spine (lumber) using a Lunar PIXImus device (GE Medical Systems, Fitchburg, WI, USA). After sacrificing animals, μCT imaging of the femur was conducted using a high-resolution μCT system (Bruker-MicroCT, Kontich, Belgium; Skyscan 1172). Scans were performed on hydrated bones with the long axis oriented vertically at an isotropic voxel size of 9.9 μm resolution (V = 60 kV, I = 167 μA), then reconstructed for cortical analysis. After reconstruction, the scans were uniformly rotated to ensure proper alignment (Dataviewer, Bruker-MicroCT). After scanning, bones

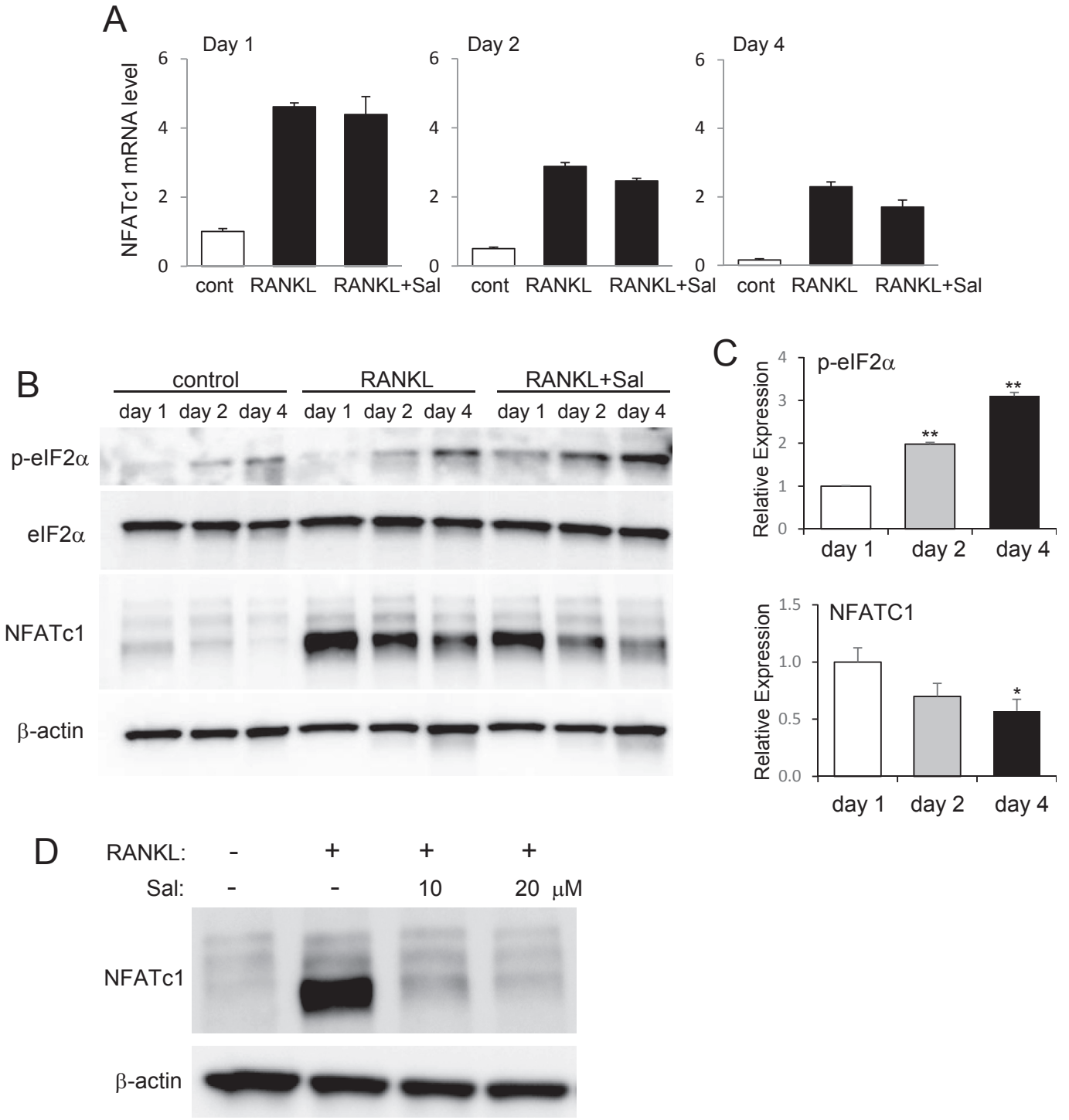

Fig. 1. Downregulation of NFATc1 by salubrinal in RAW264.7 pre-osteoclasts and bone marrow derived cells. We cultured RAW264.7 pre-osteoclasts with 50 ng/ml RANKL and 10 μM salubrinal for 1, 2, and 4 days, while bone marrow derived cells with 50 ng/ml RANKL and 10 or 20 μM salubrinal for 2 days. (A) Salubrinal-driven decrease in NFATc1 mRNA level in response to RANKL stimulation in RAW264.7 pre-osteoclasts. The mRNA level is normalized using the level for the control sample on day 1. (B & C) Elevation of the protein level of p-eIF2α and reduction in the protein level of NFATc1 by salubrinal in RAW264.7 pre-osteoclasts. The relative expression level is defined as the ratio of the level for the (RANKL + Sal) group to the level for the RANKL group, and it is normalized by the ratio on day 1. (D) Reduction in the protein level of NFATc1 by 10 or 20 μM salubrinal in bone marrow derived cells.

were wrapped in PBS-soaked gauze and stored at −20 °C until mechanical testing.

All femora were brought to room temperature and then placed in a four-point bending fixture with the mid-diaphysis positioned halfway between the loading points (support span of 9 mm, loading span of 3 mm). With the anterior surface in tension, each bone was monotonically tested to failure in displacement control at 0.025 mm/s (ElectroForce 3200, TA Instruments, New Castle, DE). The distance from the distal end of the bone to the location of fracture initiation was measured using calipers. Seven transverse slices were obtained from μCT images at the location of fracture and geometric properties (moment of inertia about the medial-lateral

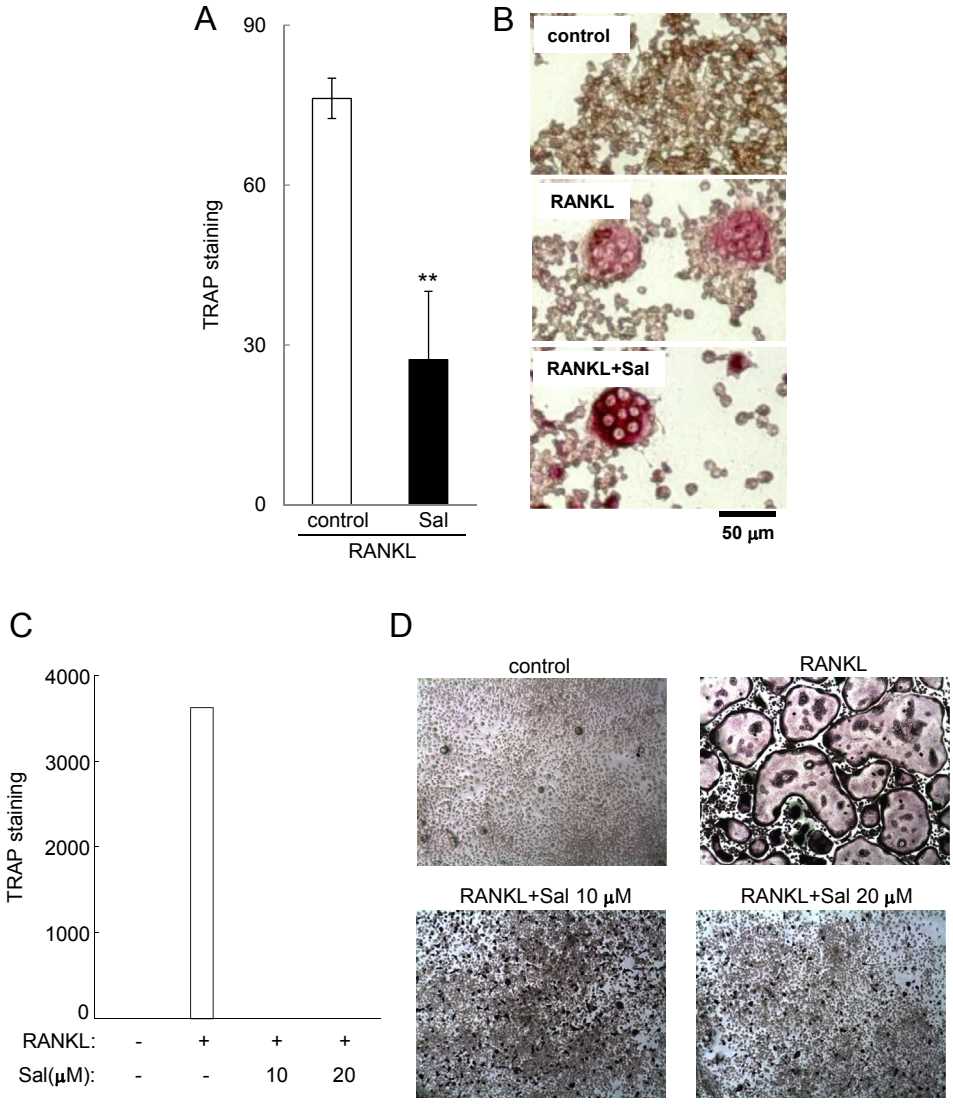

Fig. 2. Salubrinal-driven inhibition of osteoclast development in RAW264.7 pre-osteoclasts and bone marrow derived cells. We cultured RAW264.7 pre-osteoclasts with 50 ng/ml RANKL and 10 μM salubrinal for 4 days, and bone marrow derived cells with 50 ng/ml RANKL and 10 or 20 μM salubrinal for 2 days. (A) Reduction in TRAP staining by salubrinal in RAW264.7 pre-osteoclasts. The double asterisk indicates $p < 0.01$. We used 50 ng/ml RANKL without salubrinal as a control. (B) Suppression of osteoclast maturation by salubrinal in RAW264.7 pre-osteoclasts. (C) Reduction in TRAP staining by 10 or 20 μM salubrinal in bone marrow derived cells. (D) Suppression of osteoclast maturation by salubrinal in bone marrow derived cells. Of note, DMSO was employed as a vehicle control.

centroidal axis and the distance from the centroid to the extreme fiber in tension) were used to map load-displacement into stress-strain. Pre- and post-yield mechanical properties were obtained from the resulting data using a custom MATLAB script.

2.7. Statistical analysis

Three to four independent experiments were conducted, and data were expressed as mean ± S.D. Statistical significance was evaluated using ANOVA followed by post-hoc Tukey test.

3. Results

3.1. Salubrinal-driven downregulation of NFATc1 in RAW264.7 pre-osteoclasts and bone marrow derived cells

NFATc1 is a key transcription factor for activating development of osteoclasts. In response to RANKL stimulation, the mRNA level of NFATc1 was elevated 2–4 fold on days 1–4. Treatment with 10 μM salubrinal significantly suppressed RANKL-induced upregulation of NFATc1 mRNA on days 2 and 4 in RAW264.7 pre-osteoclasts (Fig. 1A). Consistent with the role of salubrinal as an inhibitor of de-phosphorylation of eIF2α, the phosphorylation level of eIF2α was elevated on days 2 and 4 in RAW264.7 pre-osteoclasts (Fig. 1B & C). Furthermore, consistent with its mRNA level the NFATc1 protein level was also suppressed on day 4 in RAW264.7 pre-osteoclasts (Fig. 1B). Furthermore, the level of NFATc1 protein in bone marrow derived cells was suppressed on day 2 (Fig. 1D).

3.2. Inhibition of osteoclast maturation by salubrinal

Besides suppression of NFATc1 expression, salubrinal reduced TRAP staining and reduced maturation of RAW264.7 pre-osteoclasts and bone marrow derived cells (Fig. 2). The number of TRAP-positive multi-nucleated cells was increased by RANKL, and

this increase was significantly suppressed by incubation with 10 or 20 μM salubrinal.

3.3. Salubrinal-driven elevation of alizarin red S staining in BMDCs

To evaluate the role of salubrinal in development of mesenchymal stem cells, we harvested BMDCs from Oim mice and mesenchymal stem cells were incubated in an osteogenic medium for 4 weeks. The level of alizarin red S staining was elevated by 5 or 10 μM salubrinal (Fig. 3).

3.4. Radiographic analysis

Radiographic measurements by DEXA for the control OI mice and salubrinal-treated OI mice showed that no significant difference was detectable in bone mineral density (BMD) in the femur, tibia, humerus, ulna, and spine (Fig. 4A). Furthermore, among three groups including the wildtype (WT) group, we did not detect clear differences in the trabecular bone thickness and tissue mineral density, as well as the cortical bone thickness and tissue mineral density in μCT images (Fig. 4B–E).

3.5. Mechanical responses of the femur

In response to a ramp input of force, the force–displacement curve was plotted and the stress–strain relationship was built for the normal wildtype, Oim placebo, and salubrinal-treated Oim groups (schematically shown in Fig. 5). These curves qualitatively show that wildtype bones were the stiffest and strongest with the greatest ductility, while the Oim placebo group had the lowest

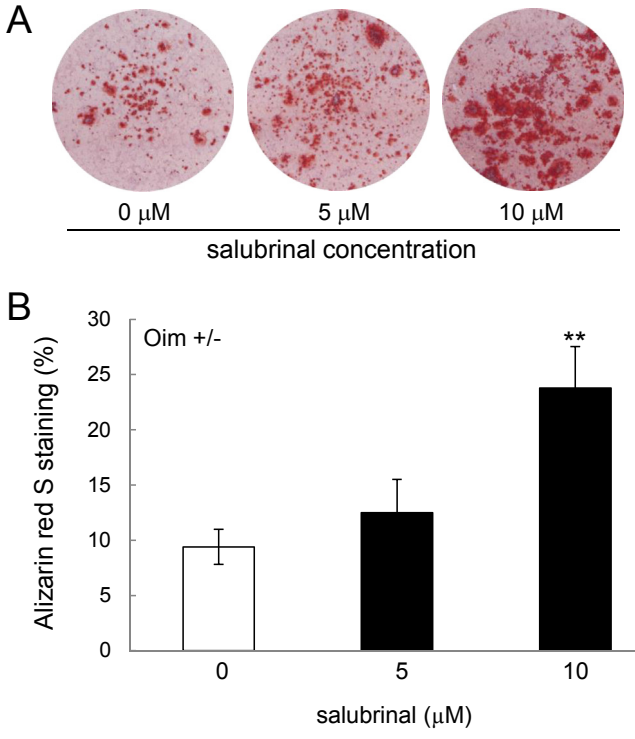

Fig. 3. Salubrinal-driven elevation of alizarin red S staining in bone marrow derived mesenchymal cells, which were isolated from heterozygous Oim mice. We cultured cells using the protocol previously developed for promoting osteoblastogenesis with 0 (control), 5, and 10 μM salubrinal for 28 days. (A) Alizarin red S staining in response to 0 (control), 5 and 10 μM salubrinal. (B) Quantification of the level of alizarin red S staining. We used 0 μM salubrinal as a control. The double asterisk indicates $p < 0.01$.

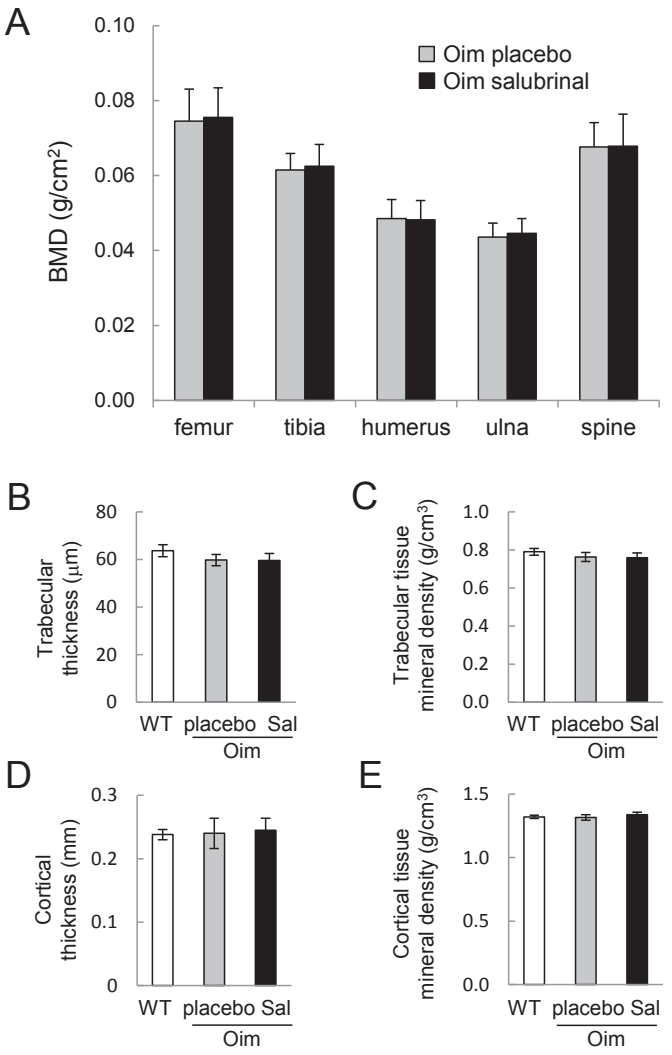

Fig. 4. Radiographic measurements. (A) Bone mineral density of the femur, tibia, humerus, ulna, and spine (L1-6) using DEXA. We used Oim placebo as a control. (B & C) Thickness and tissue mineral density of the trabecular bone using μCT. We used wildtype as a control. (D & E) Thickness and tissue mineral density of the cortical bone using μCT. We used wildtype as a control.

mechanical parameters. Treatment with salubrinal tended to beneficially impact all mechanical properties in the Oim mice.

From the responses illustrated in Fig. 5, 16 mechanical parameters were determined to evaluate the effects of salubrinal (Table 1). Among them, 2 parameters are linked to force (yield force, and ultimate force), 3 parameters to displacement (displacement to yield, post yield displacement, and total displacement), 3 parameters to energy (work to yield, post yield work, and total work), 2 parameters to strain (strain to yield, and total strain), 2 parameters to stress (yield stress, and ultimate stress), and 4 other parameters (stiffness, elastic modulus, resilience, and toughness). In all parameters, the Oim placebo group exhibited a lower value than the normal wildtype group (8 of these reached significance). In 15 out of 16 parameters except for post yield displacement, the salubrinal-treated group showed a higher value than the Oim placebo group. In 3 parameters (stiffness, elastic modulus, and total strain), the Oim placebo group means were significantly decreased relative to the wildtype group, and these differences were abolished by treatment with salubrinal (Fig. 6).

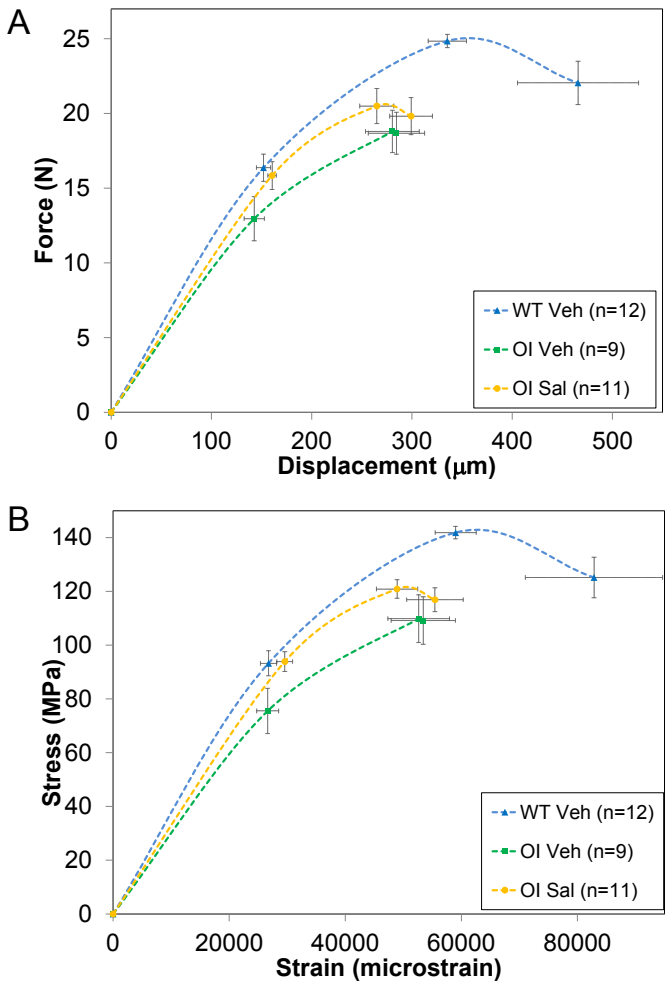

Fig. 5. Schematic representation of the mechanical responses of the femur in three animal groups. Each point represents the mean for each group (e.g., mean yield force and displacement to yield). The error bars are the standard error of the mean (SEM). Of note, WT Veh = normal wildtype control, OI Veh = Oim placebo control, and OI Sal = Oim treated with salubrinal. We used wildtype as a control. (A) Relationship between force (N) and displacement (μm). (B) Relationship between stress (MPa) and strain (μstrain).

4. Discussion

This study shows that daily administration of salubrinal to heterozygous Oim mice provides an overall tendency to improve mechanical properties of the femur of Oim mice. In 15 mechanical parameters out of 16 parameters in Table 1, the salubrinal-treated group showed the higher value than the Oim placebo group. In particular, the Oim placebo group exhibited a significantly lower value in stiffness and elastic modulus than the normal control group, while no significant difference in those values was observed between the normal control and salubrinal-treated Oim groups. The salubrinal-treated group presented the highest value in 5 parameters such as displacement to yield, work to yield, yield stress, strain to yield, and resilience, although none of those parameters showed statistical significance to the wildtype and Oim control groups at $p < 0.05$.

The current study together with our previous works on osteoblasts and osteoclasts support the notion that salubrinal's action is mediated by eIF2α signaling via the responses to the stress to the endoplasmic reticulum or protein misfolding. Protein misfolding due to collagen mutation could induce the stress to the endoplasmic reticulum and lead to osteoblast apoptosis (14,15). Salubrinal-driven elevation of phosphorylated eIF2α translationally activates the expression of ATF4, which is one of the three known transcription factor for bone formation (17). Furthermore, we have previously shown that downregulation of NFATc1, a master transcription factor for osteoclast development, is mediated by suppression of c-fos via eIF2α signaling (18). The reduction in NFATc1's protein level was steeper than that in its mRNA level. In addition to salubrinal's transcriptional regulation, this differential reduction might be linked to its translational regulation via eIF2α phosphorylation. Further analysis is necessary for a better understanding of salubrinal's action on NFATc1.

Unlike an anabolic agent such as PTH and BMPs that may present a potential risk of inducing tumors, salubrinal is shown to alleviate malignant phenotypes of chondrosarcoma (22) and mammary tumors (23). Furthermore, salubrinal activates bone remodeling as opposed to bisphosphonates acting as a suppressor of bone remodeling. Recent meta-analyses in 2008 and 2014 did not support a statistically significant effect of bisphosphonates on fractures in osteogenesis imperfecta (24,25). Bisphosphonate driven inhibition of osteoclasts without stimulating bone formation

Table 1
Mechanical parameters for three animal groups.

Parameter	Unit	Normal wildtype	Oim placebo			Oim salubrinal		
		mean ± S.D.	mean ± S.D.	Δpw (%)	p^*	mean ± S.D.	Δsp (%)	p^*
Yield force	N	16.37 ± 3.16	12.95 ± 4.44	−20.9		15.84 ± 3.09	17.7	
Ultimate force	N	24.85 ± 1.54	18.80 ± 4.25	−24.3		20.50 ± 3.89	6.8	
Displacement to yield	μm	152.00 ± 24.44	142.67 ± 30.46	−6.1		160.55 ± 13.55	11.8	
Post yield displacement	μm	313.67 ± 206.42	141.89 ± 102.33	−54.8	0.019	138.64 ± 62.80	−1.0	0.016
Total displacement	μm	465.67 ± 209.11	284.56 ± 84.44	−38.9	0.009	299.18 ± 70.68	3.1	0.018
Stiffness	N/mm	119.18 ± 12.30	97.15 ± 15.59	−18.5	0.005	106.31 ± 15.76	7.7	
Work to yield	mJ	1.33 ± 0.38	1.03 ± 0.49	−22.6		1.34 ± 0.34	23.3	
Post yield work	mJ	6.40 ± 3.69	2.38 ± 1.72	−62.8	0.002	2.59 ± 1.30	3.3	0.003
Total work	mJ	7.73 ± 3.57	3.40 ± 1.67	−56.0	0.001	3.94 ± 1.54	7.0	0.002
Yield stress	MPa	93.23 ± 16.15	75.53 ± 25.30	−19.0		93.87 ± 12.10	19.7	
Ultimate stress	MPa	141.86 ± 8.15	109.83 ± 26.52	−22.6		120.90 ± 11.31	7.8	
Strain to yield	μstrain	26,771 ± 4810	26,637 ± 5648	−0.5		28,577 ± 4480	7.2	
Total strain	μstrain	82,851 ± 40,983	53,423 ± 16,646	−35.5	0.043	55,450 ± 16,132	2.4	
Modulus	GPa	3.87 ± 0.42	3.06 ± 0.64	−20.9	0.004	3.47 ± 0.53	10.6	
Resilience	MPa	1.34 ± 0.37	1.11 ± 0.51	−17.2		1.46 ± 0.35	26.1	
Toughness	MPa	7.94 ± 4.16	3.70 ± 1.80	−53.4	0.002	4.27 ± 1.63	7.2	0.013

Δpw: %difference of the mean values ([Oim placebo − normal wildtype]/normal wildtype).
Δsp: %difference of the mean values ([salubrinal-treated Oim − Oim placebo]/normal wildtype).
* Statistically significant *p*-value with respect to the normal wildtype.

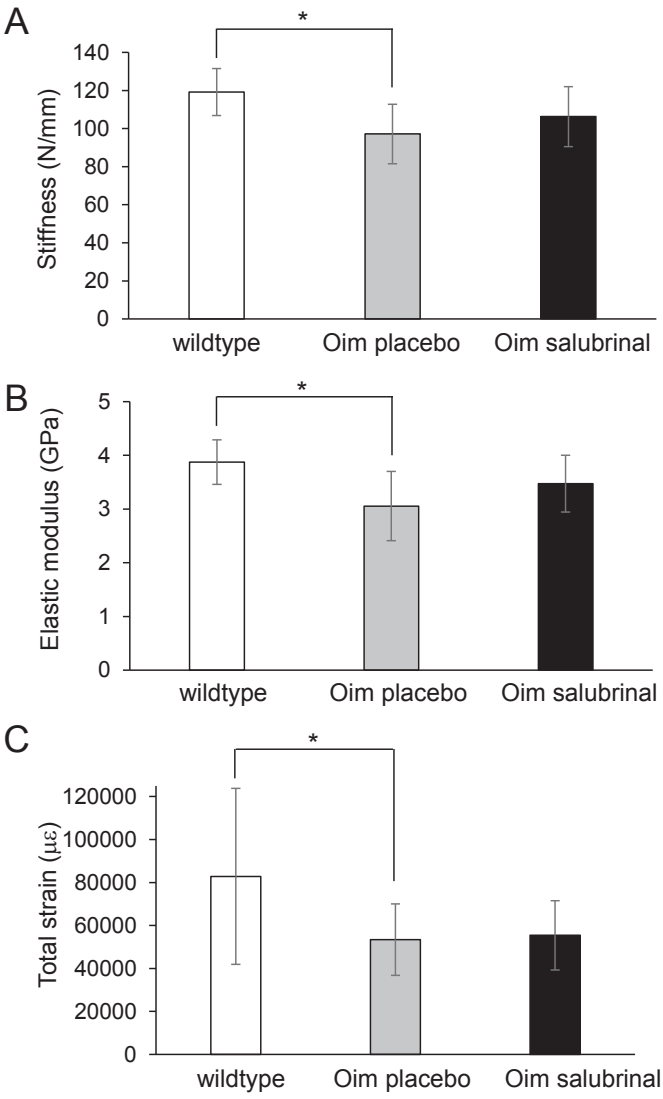

Fig. 6. Evaluation of mechanical parameters in response to salubrinal. The asterisk indicates $p < 0.05$. We used wildtype as a control. (A) Stiffness (N/mm). (B) Elastic modulus (GPa). (C) Total strain (με).

may lead to non-dynamic bone, in which microcracks are often not repaired (26). An additional potential benefit with salubrinal is its effects on cartilage, which needs to be protected from degradation without excessive bone formation. Salubrinal is able to protect cartilage degradation by suppression MMP13 activity (27,28). These suppressive effects on tumor growth and skeletal inflammation are salubrinal's unique features.

The Oim mouse model in this study exhibited a clear trend of weakened mechanical properties, but the statistically significant difference was not detected in the half of the selected parameters. The subtle differences between the normal wildtype and Oim (+/−) mice made it difficult to identify significant efficacy in salubrinal's administration to Oim (+/−) mice. Consistent with our observation, no significant difference in bone volume is reported between the normal wildtype and Oim (+/−) mice (29). Since Oim (−/−) mice present a more severe phenotype than Oim (+/−) mice, employing Oim (−/−) mice and examining their responses to salubrinal might be the next step. Alternatively, different methodologies such as Raman spectroscopy might be useful to detect subtle differences among groups. Taken together, salubrinal might potentially ameliorate Oim's damaged collagen fibrils, since it is reported that anti-sclerostin antibody, which promotes bone formation, alters bone quality (30).

Although all patients with OI present brittle bone, the genetic cause of OI differs. The murine model of OI, employed in this study, correspond to type I collagen mutation, the most frequent type of OI. Among other types of OI, types V–X are caused by mutations in IFITM5 (interferon induced transmembrane protein 5), SERPINF1 (serpin peptidase inhibitor 1), CRTAP (cartilage associated protein), LEPRE1 (leucine proline-enriched proteoglycan 1), PPIB (peptidyl prolyl cis-trans isomerase B), and SERPINH1 (serpin family H member 1), respectively (26). Therapeutic efficacy of any agent should vary depending on OI types and it is recommended to further evaluate the effects of salubrinal for other types of OI.

In this study, we employed a single dose of 2 mg/kg body weight via subcutaneous injection. It is possible that other doses at different routes and treatment durations may provide superior efficacy in improving bone quality and quantity. In summary, this study demonstrated a novel strategy for potential treatment of OI with salubrinal via regulation of eIF2α phosphorylation. The effect of salubrinal should be test on other forms of OI since the role of eIF2α signaling may differ depending on genes and regulatory steps in collagen mutation.

Conflicts of interest

The authors declare no conflict of interest.

Author contributions

Conception and experimental design: Hamamura K, Li B, Sudo A, Yokota H.

Data collection and interpretation: Takigawa S, Frondorf B, Wallace J, Liu S, Liu Y.

Drafted manuscript: Hamamura K, Wallace J, Yokota H.

Acknowledgement

This study was in part supported by Indiana Clinical and Translational Science Institute through the NIH Clinical and Translational Science Award program, grant TR000006(to HY), and NIH K25 Award (to JW). The authors do not have any competing interests.

References

(1) Eddeine HS, Dafer RM, Schneck MJ, Biller J. Bilateral subdural hematomas in an adult with osteogenesis imperfecta. J Stroke Cerebrovasc Dis. 2009;18:313–315.
(2) Rauch F, Glorieux FH. Osteogenesis imperfecta. Lancet. 2004;363:1377–1385.
(3) Aftab SA, Reddy N, Owen NL, Pollitt R, Harte A, McTernan PG, et al. Identification of a novel heterozygous mutation in exon 50 of the COL1A1 gene causing osteogenesis imperfecta. Endocrinol Diabetes Metab Case Rep 2013:130002.
(4) Cho SY, Ki CS, Sohn YB, Kim SJ, Maeng SH, Jin DK. Osteogenesis imperfecta Type VI with severe bony deformities caused by novel compound heterozygous mutations in SERPINF1. J Korean Med Sci. 2013;28:1107–1110.
(5) Mehlman CT, Shepherd MA, Norris CS, McCourt JB. Diagnosis and treatment of osteopenic fractures in children. Curr Osteoporos Rep. 2012;10:317–321.
(6) Ben Amor M, Rauch F, Monti E, Antoniazzi F. Osteogenesis imperfect. Pediatr Endocrinol Rev 2013;(Suppl. 2):397–405.
(7) Glorieux FH, Bishop NJ, Plotkin H, Chabot G, Lanoue G, Travers R. Cyclic administration of pamidronate in children with severe osteogenesis imperfecta. N Engl J Med. 1998;339:947–952.
(8) Bachrach LK, Ward LM. Clinical review 1: bisphosphonate use in childhood osteoporosis. J Clin Endocrinol Metab. 2009;94:400–409.
(9) Lewiecki EM. Safety of long-term bisphosphonate therapy for the management of osteoporosis. Drugs. 2011;71:791–814.

(10) Bargman R, Huang A, Boskey AL, Raggio C, Pleshko N. RANKL inhibition improves bone properties in a mouse model of osteogenesis imperfecta. Connect Tissue Res. 2010;51:123–131.
(11) Yamashita S. Bone and joint diseases in children. Bisphosphonates in osteogenesis imperfect. Clin Calcium. 2010;20:918–924.
(12) Bachrach LK. Consensus and controversy regarding osteoporosis in the pediatric population. Endocr Pract. 2007;13:513–520.
(13) Buevich A, Baum J. Nuclear magnetic resonance characterization of peptide models of collagen-folding diseases. Philos Trans R Soc Lond B Biol Sci. 2001;356:159–168.
(14) Hamamura K, Liu Y, Yokota H. Microarray analysis of thapsigargin – induced stress to the endoplasmic reticulum of mouse osteoblasts. J Bone Min Metab. 2008;26:231–240.
(15) Lisse TS, Thiele F, Fuchs H, Hans W, Przemeck GK, Abe K, et al. ER stress-mediated apoptosis in a new mouse model of osteogenesis imperfecta. PLoS Genet. 2008;4:e7.
(16) Boyce M, Bryant KF, Jousse C, Long K, Harding HP, Scheuner D, et al. A selective inhibitor of eIF2α dephosphorylation protects cells from ER stress. Science. 2005;332:91–94.
(17) Hamamura K, Tanjung N, Yokota H. Suppression of osteoclastogenesis through phosphorylation of eukaryotic translation initiation factor 2 alpha. J Bone Min Metab. 2013;31:618–628.
(18) Hamamura K, Chen A, Tanjung N, Takigawa S, Sudo A, Yokota H. *In vitro* and *in silico* analysis of an inhibitory mechanism of osteoclastogenesis by salubrinal and guanabenz. Cell Signal. 2015;27:353–362.
(19) Yokota H, Hamamura K, Chen A, Dodge TR, Tanjung N, Abedinpoor A, et al. Effects of salubrinal on development of osteoclasts and osteoblasts from bone marrow-derived cells. BMC Musculoskelet Disord. 2013;14:197.
(20) Rachner TD, Khosla S, Hofbauer LC. Osteoporosis: now and the future. Lancet. 2011;377:1276–1287.
(21) Mazziotti G, Bilezikian J, Canalis E, Cocchi D, Giustina A. New understanding and treatments for osteoporosis. Endocrine. 2012;41:58–69.
(22) Xu W, Wan Q, Na S, Yokota H, Yan J, Hamamura K. Suppressed invasive and migratory behaviors of SW1353 chondrosarcoma cells through the regulation of Src, Rac1 GTPase, and MMP13. Cell Signal. 2015;27:2332–2342.
(23) Hamamura K, Minami K, Tanjung N, Wan Q, Koizumi M, Matsuura N, et al. Attenuation of malignant phenotypes of breast cancer cells through eIF2α-mediated downregulation of Rac1 signaling. Int J Oncol. 2014;44:1980–1988.
(24) Phillipi CA, Remmington T, Steiner RD. Bisphosphonate therapy for osteogenesis imperfecta. Cochrane Database Syst Rev. 2008;8:CD005088.
(25) Dwan K, Phillipi CA, Steiner RD, Basel D. Bisphosphonate therapy for osteogenesis imperfecta. Cochrane Database Syst Rev. 2014;7:CD005088.
(26) Forlino A, Marini JC. Osteogenesis imperfecta. Lancet. 2016;387:1657–1671.
(27) Hamamura K, Lin C-C, Yokota H. Salubrinal reduces expression and activity of MMP13 in chondrocytes. Osteoarthr Cartil. 2013;21:764–772.
(28) Hamamura K, Nishimura A, Iino T, Takigawa S, Sudo A, Yokota H. Chondroprotective effects of Salubrinal in a mouse model of osteoarthritis. Bone Joint Res. 2015;4:84–92.
(29) Saban J, Zussman MA, Havey R, Patwardhan AG, Schneider GB, King D. Heterozygous oim mice exhibit a mild form of osteogenesis imperfecta. Bone. 1996;19:575–579.
(30) Ross RD, Edwards LH, Acerbo AS, Ominsky MS, Virdi AS, Sena K, et al. Bone matrix quality after sclerostin antibody treatment. J Bone Min Res. 2014;29:1597–1607.